

Chapter 13

High-Pressure Studies with Microdiffraction

HPSTAR
044-2014

Wenge Yang

*High Pressure Synergetic Consortium,
Geophysical Laboratory,
Carnegie Institution of Washington,
Argonne, IL 60490, USA
wyang@ciw.edu*

As one of the fundamental state parameters, pressure plays an essential role in a material's structural stability, electronic structure, magnetic transition and in the formation of new materials which cannot be synthesized at ambient condition. Materials subjected to mechanical or energetic particles often fail at one-tenth or less of their intrinsic limits, and we still do not fully understand the micromechanism for this. Reaching the intrinsic limit of materials performance requires understanding of the microstructural response under extreme conditions. Formation and movement of defects can be driven by external stress and temperature. *In situ* probing the deformed microstructure in a real condition at micro-/nanoscale will dramatically improve our understanding of materials processes. Stress often alerts the material response dramatically near phase transition, especially under significant shear stress conditions. Multiple phases in composite materials and pressure gradient induced inhomogeneity and require a small volume probe to get local structural information. Since the X-ray microdiffraction technique was first introduced to the high-pressure community, it has been widely utilized to solve the above-mentioned problems. In this chapter, we will give a brief overview of applications of microdiffraction to high-pressure research.

13.1. Introduction

Typically there are two types of high-pressure devices: large volume press (LVP) and diamond anvil cell (DAC). The LVP uses multi-anvil design to

compress samples at the order of centimeter length scale. Coupling with resistivity heating, LVP provides important access for Earth science studies with pressure up to 30 GPa and temperature to 3000 K (Weidner *et al.*, 1992; Zhao *et al.*, 1992; Uchida *et al.*, 2002; Chen *et al.*, 2004). DAC on the other hand, is the major tool used to study much higher-pressure and temperature-range phenomena (a few mK to 6000 K) with specialized cryostat and heating devices (Mao *et al.*, 2001; Eremets and Troyan, 2011; Guillaume *et al.*, 2011; Huang *et al.*, 2011; Murakami *et al.*, 2012; Sun *et al.*, 2012). Conditions of the Earth's center (364 GPa and 5500°C) were recreated in the lab using DAC (Hirose and Ohishi, 2010). As shown in Fig. 13.1a, LVP can supply thousands of tons of force to a large bulk sample from millimeter to centimeter size. Typically, 6 or 8 tungsten carbide (WC) anvils are used to compress a sample uniaxially or hydraulically. For DACs, typical anvil culet sizes are from several to hundreds of micrometers in diameter, and a gasket is used to create sample chamber between two anvils. Figures 13.1b and 13.1c show the two commonly used DACs, named panoramic DAC

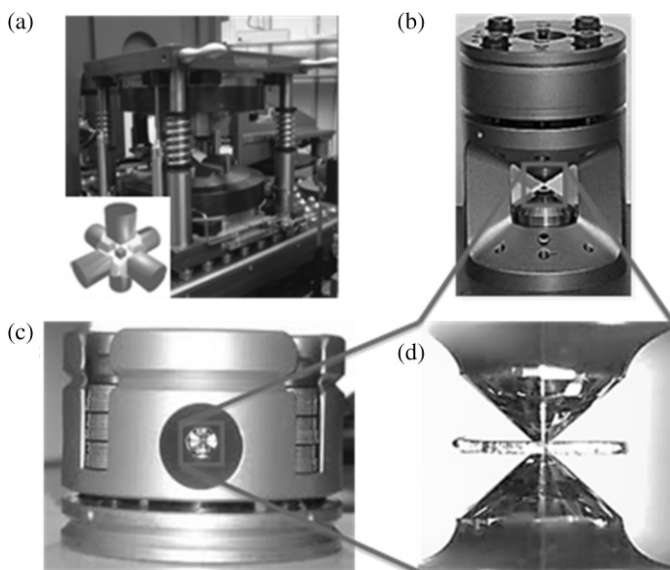


Fig. 13.1. Two types of typical high-pressure devices. (a) The LVP; (b) a two-fold design panoramic DAC; (c) a symmetrical DAC; and (d) a zoomed-in view of the diamond anvils and sample chamber.

and symmetric DAC. The zoomed-in anvil tip and gasket part are shown in Fig. 13.1d.

Pressure drastically changes materials' properties (Bridgman, 1949; Basic Research Needs MuEE, 2007). High-pressure structure study has been largely promoted with synchrotron-based diffraction techniques.

The quality of measurement under compression is governed by the size of analytical probe relative to the size of the samples. The standard submicron scale probes using focused electrons, ions or surface contact techniques require a low-pressure environment (or near vacuum), and the probe particles (electrons and ions) will be largely absorbed by diamond windows. Optical probes are often used to access the high-pressure sample through diamond windows with the limitation to about $1\ \mu\text{m}$ due to the diffraction limit of the optical wavelength. High energy X-rays have been utilized as a powerful tool to probe the high-pressure sample through diamond windows or X-ray transparent (for example, beryllium) gaskets for *in situ* studies. Hard X-ray diffraction (XRD) with the short wavelength and large penetration depth has been the primary probe tool for high-pressure research. The availability of microdiffraction plays the key role on the ultra-high-pressure research, for instance, in determining new high-pressure phases (Vailionis *et al.*, 2011), inhomogeneity of sample (Ding *et al.*, 2012), stress/strain gradient (Klepeis *et al.*, 2010), texture evolution (Merkel *et al.*, 2007) and so on.

13.2. Ultra-High Pressure and Pressure Gradient

As pressure is defined as force per unit area, the higher the pressure, the smaller the sample area one can apply. Typically, high-pressure diffraction beamlines have a focused beamsizes of around $5\text{--}20\ \mu\text{m}$ (full width at half medium (FWHM)). For ultra-high pressure (multi-megabar), the culet size is about $10\text{--}20\ \mu\text{m}$ (Wang *et al.*, 2010). In such cases, it is hard to get clean data without gasket contamination.

Figure 13.2 shows one application where $18\ \mu\text{m}$ culet-size diamond anvil and multiple samples were loaded in the same sample chamber. With a $600\ \text{nm}$ focused beamsizes, one can clearly distinguish the absorption contrast from Fe, Pt and W in Fig. 13.2a. The circular ring shadow outside of the sample chamber indicates the gasket absorption. For such an application,

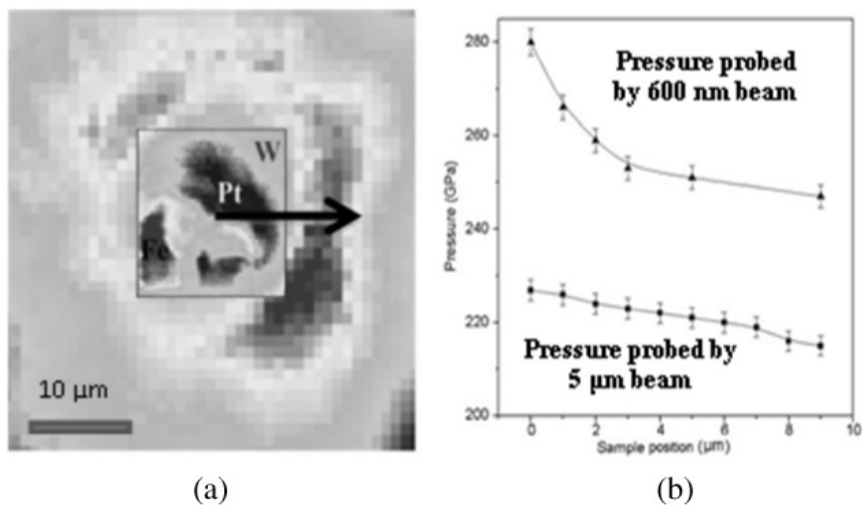


Fig. 13.2. Microdiffraction on ultra-high-pressure sample. Two-dimensional (2D) absorption map of multiple samples in a symmetrical DAC (a) and the pressure gradient measured with 600 nm and 5 μm beamsizes (b).

we performed the microdiffraction comparison with both 5 μm and 600 nm beamsizes from the center of the culet to the outside of the gasket, as indicated by the black arrow. Based on the known samples' equation of state, one can determine the pressure at the probed location. Figure 13.2b displays the pressures measured with two different beamsizes. There is a sharp pressure drop from the center of the culet to the edge from the submicron beam diffraction, but it is not sensitive from the 5 μm beamsizes diffraction. It is important to measure the crystalline structure information at a narrow pressure range, especially for those structural transitions at the ultra-high-pressure region as often the high-pressure phase is mixed with a low-pressure phase and it is hard to determine the transition boundary. With submicron beam diffraction capabilities, we expect to get clean diffraction data at pressure towards the diamond limit.

13.3. Radial Diffraction and Material Strength Measurement

Most commonly used pressure media (liquid methanol–ethanol mixture; argon, neon, helium gases) will be frozen above 12 GPa, and only provide a quasi-hydraulic pressure environment for samples. Routinely, DAC can

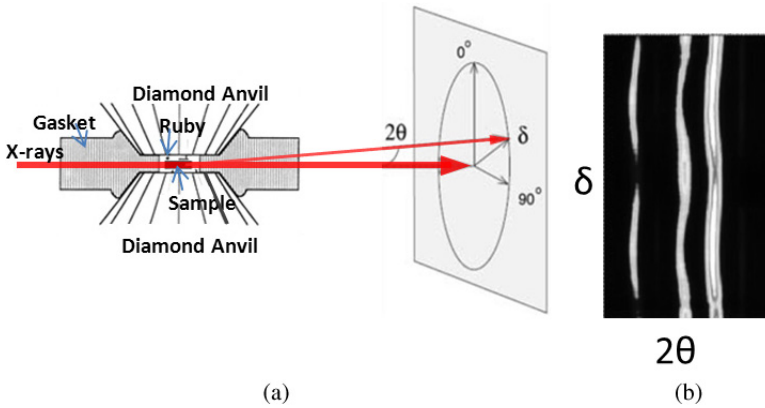


Fig. 13.3. High pressure radial diffraction setup. (a) the diamond anvil, sample and detector configuration; (b) typical integrated intensity as a function of 2θ and azimuth angle δ with large elastic anisotropy.

provide pressure to several hundred gigapascals. Most materials have large anisotropic elastic behavior, which will respond quite differently under external stress along different lattice planes. This property can be used to measure the elastic constants under uniaxial compression by utilizing the so-called radial diffraction method (Chesnut *et al.*, 2006; Merkel *et al.*, 2007; Kavner, 2008; Klepeis *et al.*, 2010). The experimental setup is illustrated in Fig. 13.3. Instead of penetrating through the diamond windows, the X-rays go through a light element gasket (like beryllium) and an area detector is used to record the 2D diffraction patterns. The diffraction ring for the same lattice d_{hkl} will look like the wavy curve along the azimuth angle δ , which means this lattice parameter changes at different δ angle. The lattice d-spacing measured with radial diffraction follows the equation:

$$d_m(hkl) = d_p(hkl)[1 + (1 - 3 \cos^2 \delta) Q(hkl)] \quad (13.1)$$

where $d_m(hkl)$ is the measured d-spacing at azimuth angle δ , $d_p(hkl)$ is the hydrostatic d-spacing, which is usually used for equation of state measurement, δ is the azimuth angle and $Q(hkl)$ is a function of the elastic constants. At the magic angle $\delta = 54.74^\circ$, $d_m(hkl) = d_p(hkl)$ and the deviatoric stresses will be removed from the data. In order to apply

Eq. 13.1 to radial diffraction data, the sample chamber needs to be very small compared to the diamond culet, and the probing beam also needs to be small. The limitation of Eq. 13.1 has been addressed by Matthies *et al.* (2001).

The pressure gradient along the radial direction is largely related to the material shear stress σ_{rz} . The yield stress, Y , is considered as twice of the shear stress, σ_{rz} (Klepeis *et al.*, 2010) and follows the following approximation:

$$Y = 2\sigma_{rz} \approx h(dP/dr) \quad (13.2)$$

Here h is the sample thickness and dP/dr is the pressure gradient along the radial direction. The measurements of sample thickness and pressure across the radial direction can be performed by combining micro-beam absorption and diffraction methods. Typically, the sample thickness is around $20 \mu\text{m}$ and the X-ray energy is above 20 keV. The thickness can be calculated based on the density absorption of the studied sample as:

$$h = \log(I_0/I_1)/(\mu\rho) \quad (13.3)$$

Here the I_0 and I_1 are the X-ray intensities before and after the sample is monitored by two ion chambers, and μ is the mass absorption coefficient and the ρ sample density. Furthermore, μ is a constant at a fixed X-ray energy, and ρ changes with pressure and can be calculated based on the unit cell volume obtained from diffraction data. This method was first proposed by Meade and Jeanloz (1988) on MgO, and followed by Klepeis *et al.* (2010).

13.4. Microdiffraction on Course Grain Powder Sample

High-pressure diffraction usually uses either angle-dispersive X-ray diffraction (ADX) with monochromatic beam and area detector or energy-dispersive X-ray diffraction (EDXD) with white-beam and point detector. Both methods can be used for powder or single-crystal structural determination. For powder diffraction, one needs fine grain size to obtain good statistic diffraction intensity; for single-crystal diffraction, on the other hand, preferably only one grain is illuminated by the incident X-ray beam. Often, we encounter course grain powder. In those cases, one cannot get

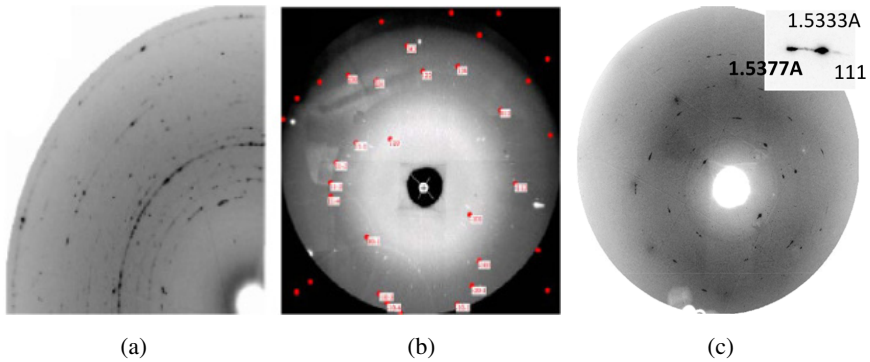


Fig. 13.4. Comparison between large beam and micro-beam diffraction on high pressure samples. A regular $5\ \mu\text{m}$ beam powder diffraction and submicron white-beam Laue diffraction on the same coarse powder sample are shown in (a) and (b), respectively. Submicron beam diffraction can also probe the two variants of rhombohedral distorted domains from the same sample.

reliable powder diffraction intensity, nor single-crystal diffraction with several microns beamsize. With a switchable white/monochromatic beam setup, one can combine both white-beam Laue diffraction and energy scan to achieve full information of individual grains (Ice *et al.*, 2005). Another approach is rotating the sample along the axis perpendicular to the incident beam, and combining the monochromatic angle-dispersive diffraction data at many angles to extract structural and deformation information (Nisar *et al.*, 2012). Inserting coarse powder sample to submicron beamsizes, one can pick up only a few grains to study the crystalline symmetry and refine the intensity. As an example shown in Fig. 13.4, the regular $5\ \mu\text{m}$ beamsizes powder diffraction on a calcium sample in a DAC shows a very spotty pattern (Fig. 13.4a). When we put the same sample into a microdiffraction beamline, we only observed a few diffraction spots, which indicated only a few grains were illuminated by the X-rays.

Switching to white beam, we can identify the Laue pattern from one grain as indexed in Fig. 13.4(b), which allowed us to study the space-group and lattice parameters. Calcium has been reported to have the highest critical temperature among elemental superconductors, but the structure keeps at a simple cubic lattice up to 119 GPa, which is not favorable for the total energy minimization. The application of microdiffraction to the

calcium sample under high pressure for the first time confirms the structure undergoes a simple cubic to rhombohedral distortion by distinguishing the small deviation of lattice parameters from the two adjacent domains, as shown in the insert of Fig. 13.4c (Mao *et al.*, 2010). In powder diffraction, one can only expect a small peak broadening effect, which is not enough to identify the new phases. With much higher d-spacing resolution from the single-crystal diffraction method, it may come to routine procedure to identify the small change for submicron scale domains in high-pressure research. By making a raster scan on the micron scale single or multigrains, one can also view the diffraction contrast image by selecting one reciprocal lattice, similar to the transmission electron microscope (TEM) bright/dark field imaging. The applications to a twin domain and nanobelt show the advantage of the microdiffraction technique clearly (Wang *et al.*, 2011; Ding *et al.*, 2012).

13.5. Three-Dimensional Orientation and Strain Mapping of Diamond Anvils Under High Pressure Using DAXM

In Chapter 2, we introduced the differential aperture X-ray microscopy (DAXM) technique to gain submicron spatial resolution along the X-ray penetration direction (Larson *et al.*, 2002). This method can be applied to DAC studies too. Under ultra-high pressure, the anvils themselves are under extreme strain and strain gradient. Understanding the strain and lattice orientation distribution in both anvils near the tips will provide us with important guidance to optimize the anvil design so that we can reach an even higher pressure limit. We have adapted the DAXM configuration for allowing the differential wire to access the inside of the DAC and scan the wire in the horizontal plan just above the beryllium gasket, as shown in the upper left corner of Fig. 13.5. The beryllium gasket is 3 mm in diameter, the wire used is around $250\ \mu\text{m}$ in diameter, and detector is set at 500 mm above the sample. By moving the wire with $1\ \mu\text{m}$ step size, one can obtain $2\ \mu\text{m}$ depth resolution. As one can expect, the anvils under 55 GPa have enormous elastic strain and lattice bending. Four typical white-beam Laue patterns at four sides of the anvil are shown in Fig. 13.5 — the highlighted dots represent the locations where the DAXM is run. The DAXM scans were applied to the central line, which created

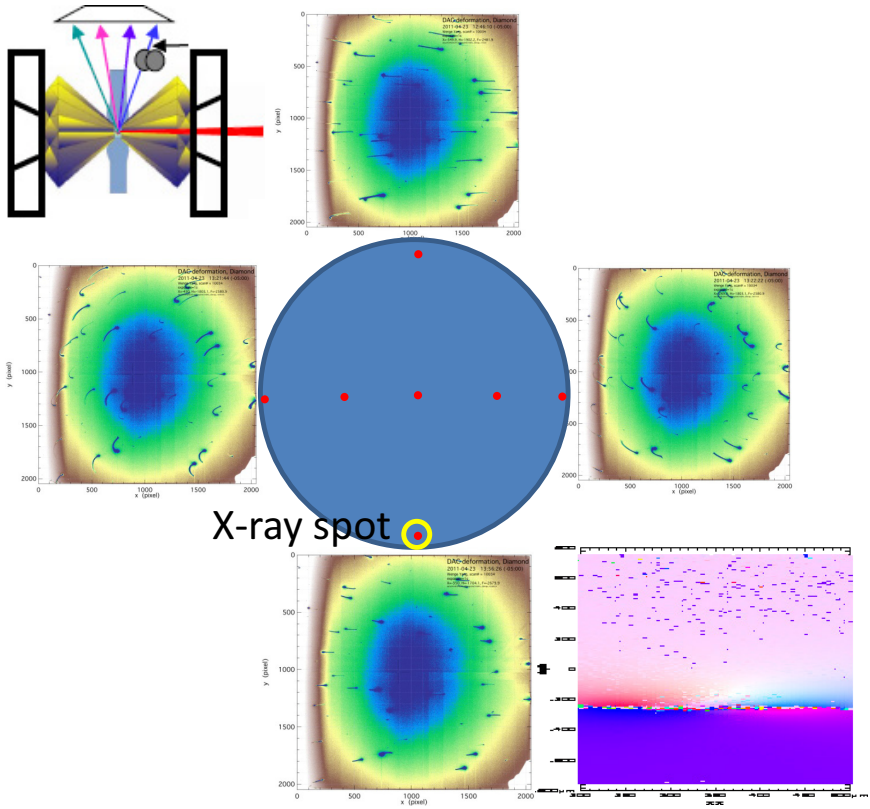


Fig. 13.5. A DAXM application to diamond anvil orientation and strain distribution mapping under high pressure. Upper left: the experimental configuration, including a differential wire moving above the beryllium gasket and an area detector for collecting 2D Laue diffraction patterns. Center: the X-ray probed locations on the anvil surface; four typical diffraction patterns at four edges of anvil showing a large lattice rotation of diamond anvil under 55 Gpa maximum pressure near the center of the anvil. Lower right: the 2D orientation map of both anvils under 55 GPa pressure.

a cross section plan through the highest pressure center. The orientation map of the surface normal (001) direction is shown in the lower-right corner. From that, one can see clearly the rotation center of the two anvils.

The unindexed line between two anvils indicated the gap from the beryllium gasket. Fitting the measured curvature to a finite element method, one can calculate the local strain distribution, and understand the critical

point when the diamond anvil breaks. This will provide the necessary revolutionary information for next-generation diamond anvil design to reach new pressure limits.

13.6. Outlook

Submicron beam X-ray diffraction is a powerful tool for modern ultra-high-pressure research. It provides us with a great tool with which to study the microstructure of materials under extreme condition in the following:

1. Multiple samples in the sample chamber;
2. Detailed mapping of strain gradient;
3. Higher resolution of lattice parameter determination;
4. Single-crystal study in a coarse powder sample.

Coupled with the newly developed three-dimensional (3D) DAXM method, one can expect to study the detailed microstructure at interfaces between different oriented crystals and/or different phases, the solid–liquid interface during the melting process and chemical reaction under extreme conditions. This technique would be especially useful to probe the evolution of microstructure during pressure-induced phase transition, and pressure-induced lattice/orbit/spin ordering. With the continuous development on the micro-/nanoscale diffraction methods, we expect to achieve atomic-scale understanding of materials responses under extreme conditions.

Acknowledgments

HPSynC is supported as part of EFree, an Energy Frontier Research Center funded by the U.S. Department of Energy, Office of Science, Office of Basic Energy Science under Award DE-SC0001057.

References

- Basic Research Needs MuEE (2007). *Report of the Basic Energy Sciences Workshop on Materials under Extreme Environments*. Available at: http://science.energy.gov/~media/bes/pdf/reports/files/muee_rpt.pdf. [Accessed 21 March 2012.]
- Bridgman, P.W. (1949). *The Physics of High Pressure*, London: G. Bell.

- Chen, J., Li, L., Weidner, D.J. and Vaughan, M.T. (2004). Deformation experiments using synchrotron X-rays: In situ stress and strain measurements at high pressure and temperature, *Phys. Earth Planet. In.*, **143**, 347–356.
- Chesnut, G.N., Schiferl, D., Streetman, B.D. and Anderson, W.W. (2006). Diamond-anvil cell for radial X-ray diffraction, *J. Phys.- Condens. Mat.*, **18**, S1083.
- Ding, Y., Cai, Z., Hu, Q., Sheng, H., Chang, J., Hemley, R.J. and Mao, W.L. (2012). Nanoscale diffraction imaging of the high-pressure transition in Fe_{1-x}O , *Appl. Phys. Lett.*, **100**, 041903.
- Eremets, M.I. and Troyan, I.A. (2011). Conductive dense hydrogen, *Nat. Mater.*, **10**, 927–931.
- Guillaume, C.L., Gregoryanz, E., Degtyareva, O., McMahon, M.I., Evans, S., Hanfland, M., Guthrie, M., Sinogeikin, S.V. and Mao, H.K. (2011). Cold melting and solid structures of dense lithium, *Nat. Phys.*, **7**, 211–214.
- Hirose, K. and Ohishi, Y. (2010). *World's First Realization of the Ultrahigh-Pressure High-Temperature Conditions at the Earth's Center in a Laboratory — Enabling the Artificial Synthesis of All Materials Existing in the Earth's Interior (Press Release)*. Available at: http://www.spring8.or.jp/en/news_publications/press_release/2010/100405. [Accessed 24 February 2013.]
- Huang, H., Fei, Y., Cai, L., Jing, F., Hu, X., Xie, H., Zhang, L. and Gong, Z. (2011). Evidence for an oxygen-depleted liquid outer core of the Earth, *Nature*, **479**, 513–516.
- Ice, G.E., Dera, P., Liu, W. and Mao, H.H. (2005). Adapting polychromatic X-ray microdiffraction technique to high-pressure research: energy scan approach, *J. Synchrotron Radiat.*, **12**, 608–617.
- Kavner, A. (2008). Radial diffraction strength and elastic behavior of CaF_2 in low- and high-pressure phases, *Phys. Rev. B*, **77**, 224102.
- Klepeis, J.H.P., Cynn, H., Evans, W.J., Rudd, R.E., Yang, L.H., Liermann, H.P. and Yang, W. (2010). Diamond anvil cell measurement of high-pressure yield strength of vanadium using *in situ* thickness determination, *Phys. Rev. B*, **81**, 134107.
- Larson, B.C., Yang, W., Ice, G.E., Budai, J.D. and Tischler, J.Z. (2002). Three dimensional X-ray structural microscopy with submicrometre resolution, *Nature*, **415**, 887–890.
- Mao, W.L., Wang, L., Ding, Y., Yang, W., Liu, W., Kim, D.Y., Luo, W., Ahuja, R., Meng, Y., Sinogeikin, S., Shu, J. and Mao, H.K. (2010). Distortions and stabilization of simple-cubic calcium at high pressure and low temperature, *PNAS*, **107**, 9965–9968.

- Mao, H.K., Xu, J., Struzhkin, V.V., Shu, J., Hemley, R.J., Sturhahn, W., Hu, M., Alp, E., Vocadlo, L., Alfè, D., Price, G.D., Gillan, M.J., Schwoerer-Böhning, M., Häusermann, D., Eng, P., Shen, G., Giefers, H., Lübbers, R. and Wortmann, G. (2001). Phonon density of states of iron up to 153 GPa, *Science*, **292**, 914–916.
- Matthies, S., Merkel, S., Wenk, H.R., Hemley, R.J. and Mao, H.K. (2001). Effects of texture on the determination of elasticity of polycrystalline iron from diffraction measurements, *Earth Planet. Sc. Lett.*, **194**, 201–212.
- Meade, C. and Jeanloz, R. (1988). Yield strength of MgO to 40 GPa, *J. Geophys. Res.*, **93**, 3261–3269.
- Merkel, S., Mcnamara, A.K., Kubo, A., Speziale, S., Miyagi, L., Meng, Y., Duffy, T.S. and Wenk, H.R. (2007). Deformation of (Mg,Fe)SiO₃ post-perovskite and D'' anisotropy, *Science*, **316**, 1729–1732.
- Murakami, M., Ohishi, Y., Hirao, N. and Hirose, K. (2012). A perovskitic lower mantle inferred from high-pressure, high-temperature sound velocity data, *Nature*, **485**, 90–94.
- Nisr, C., Ribárik, G., Ungár, T., Vaughan, G.B.M., Cordier, P. and Merkel, S. (2012). High resolution three-dimensional X-ray diffraction study of dislocations in grains of MgGeO₃ post-perovskite at 90 GPa, *J. Geophys. Res.*, **117**, B03201.
- Sun, L., Chen, X.J., Guo, J., Gao, P., Huang, Q.-Z., Wang, H., Fang, M., Chen, X., Chen, G., Wu, Q., Zhang, C., Gu, D., Dong, X., Wang, L., Yang, K., Li, A., Dai, X., Mao, H.K. and Zhao, Z. (2012). Re-emerging superconductivity at 48 K in iron chalcogenides, *Nature*, **483**, 67–69.
- Uchida, T., Wang, Y., Rivers, M.L., Sutton, S.R., Weidner, D.J., Vaughan, M.T., Chen, J., Li, B., Secco, R.A., Rutter, M.D. and Liu, H. (2002). A large-volume press facility at the advanced photon source: diffraction and imaging studies on materials relevant to the core of planetary bodies, *J. Phys. - Condens. Mat.*, **14**, 11517–11523.
- Vailionis, A., Gamaly, E.G., Mizeikis, V., Yang, W., Rode, A.V. and Juodkazis, S. (2011). Evidence of superdense aluminium synthesized by ultrafast microexplosion, *Nat. Comm.*, **2**, 445.
- Wang, L., Ding, Y., Patel, U., Yang, W., Xiao, Z., Cai, Z., Mao, W.L. and Mao, H.K. (2011). Studying single nanocrystals under high pressure using an X-ray nanoprobe, *Rev. Sci. Instr.*, **82**, 043903.
- Wang, L., Ding, Y., Yang, W., Liu, W., Cai, Z., Kung, J., Shu, J., Hemley, R.J., Mao, W.L. and Mao, H.K. (2010). Nanoprobe measurements of materials at megabar pressures, *PNAS*, **107**, 6140–6145.

- Weidner, D.J., Vaughan, M.T., Ko, J., Wang, Y., Leinenweber, K., Liu, X., Yeganeh-Haeri, A., Pacalo, R.E. and Zha, Y. (1992). Large volume high pressure research using the wiggler port at NSLS, *High Pressure Res.*, **8**, 617–623.
- Zhao, Y., Weidner, D.J., Parise, J.B. and Cox, D.E. (1992). Critical phenomena and phase transition of perovskite- data for NaMgF_3 perovskite. Part (II), *Phys. Earth Planet. In.*, **76**, 17–34.